

Nucleotide correlations and electronic transport of DNA sequences

E. L. Albuquerque,¹ M. S. Vasconcelos,² M. L. Lyra,³ and F. A. B. F. de Moura³

¹*Departamento de Física, Universidade Federal do Rio Grande do Norte, 59072-970 Natal-RN, Brazil*

²*Departamento de Ciências Exatas, Centro Federal de Educação Tecnológica do Maranhão, 65025-001 São Luís-MA, Brazil*

³*Departamento de Física, Universidade Federal de Alagoas, 57072-970 Maceió-AL, Brazil*

(Received 20 October 2004; published 23 February 2005)

We use a tight-binding formulation to investigate the transmissivity and wave-packet dynamics of sequences of single-strand DNA molecules made up from the nucleotides guanine *G*, adenine *A*, cytosine *C*, and thymine *T*. In order to reveal the relevance of the underlying correlations in the nucleotides distribution, we compare the results for the genomic DNA sequence with those of two artificial sequences: (i) the Rudin-Shapiro one, which has long-range correlations; (ii) a random sequence, which is a kind of prototype of a short-range correlated system, presented here with the same first-neighbor pair correlations of the human DNA sequence. We found that the long-range character of the correlations is important to the persistence of resonances of finite segments. On the other hand, the wave-packet dynamics seems to be mostly influenced by the short-range correlations.

DOI: 10.1103/PhysRevE.71.021910

PACS number(s): 87.14.Gg, 87.15.Aa, 72.15.Rn, 89.75.Da

I. INTRODUCTION

The field of nanotechnology has emerged as one of the most important areas of research in the near future. While scientists have been long aspiring to controllably and specifically manipulate structures at the micrometer and nanometer scale, nature has been performing these tasks and assembling structures with great accuracy and high efficiency using specific biological molecules such as DNA and proteins [1,2].

Recently, the electric conductance of DNA molecules was studied using a tight-binding small-polaron model and the length dependence of the electric current was derived [3]. It has been conjectured that the drift of polaron states may lead to a rapid motion of charges introduced on DNA [4]. However, although the use of DNA molecules in nanoelectronic circuits is a very promising task due to their self-assembly and molecular recognition abilities, their conductivity properties are still under intense debate. Controversial reports consider that DNA may be a good linear conductor [5,6], while others have found that it is somewhat more effective than proteins, even when the molecules had perfectly ordered base pairs [7–9]. Recently, measurements of electrical transport through individual short DNA molecules indicated that it has a wide-band-gap semiconductor behavior [10]. In addition, strongly deformed DNA molecules deposited on a substrate and connected to metallic electrodes can behave as an insulator or a conductor depending on the ratio between the thickness of the substrate and the molecule [11].

On the other hand, the introduction of long-range correlations in aperiodic or genomic DNA sequences markedly changes their physics and can play a crucial role in their charge transfer efficiency, making a strong impact on their biological engineering processes like gene regulation and cell division [12,13]. Moreover, the nature of this long-range correlation has been the subject of intense investigation, and its possible applications on electronic delocalization in the one-dimensional Anderson model have been recently discussed [14,15].

A DNA chain is a sequence of four possible nucleotides which define the structure of the amino acids to form proteins. Thus the DNA nucleotide sequences can be considered as a symbolic sequence of a four-letter alphabet, namely, guanine (*G*), adenine (*A*), cytosine (*C*), and thymine (*T*). Unlike proteins, a π -stacked array of DNA base pairs made up from these nucleotides can provide the way to promote long-range charge migration, which in turn gives important clues to mechanisms and biological functions of transport [16].

Numerous algorithms have been introduced to characterize and graphically represent the genetic information stored in the DNA nucleotide sequence. The goal of these methods is to generate representative pattern for certain sequences, or groups of sequences. With this aim in mind, we report in this work a numerical study of electronic conduction in arrays of DNA single-strand segments, made up from four nucleotides following either a Rudin-Shapiro quasiperiodic sequence, which has a long-range pair correlation, or a random sequence with short-range pair correlations. For comparison we show also the electrical transport properties for a genomic DNA sequence considering a segment of the first sequenced human chromosome 22 (Ch22).

This paper is structured as follows. We present in Sec. II our theoretical model based on an electronic tight-binding Hamiltonian suitable to describe a single strand of DNA segments with pure diagonal correlated disorder modeled by a quasiperiodic chain of Rudin-Shapiro (RS) type. Then we introduce another artificial structure to model the DNA molecule but with short-range correlation, namely, the pair-correlated (PC) sequence structure. Their statistical properties, like the so-called Hurst exponent, are then discussed. Section III deals with the conductivity of the DNA molecule models through their electron transmittance coefficient. Solving numerically a time-dependent Schrödinger equation, we compute also the time dependence of the *spread* of the wave function, as a function of time, for all DNA models considered here. Finally, the conclusions of this work are presented in Sec. IV.

TABLE I. Fraction of all possible first-neighbor pairs in the segment of 2000 nucleotides of the Ch22 chromosome that starts from the 100 000th one. The pair-correlated sequence is constructed to have the same conditional probabilities $P(J,I)=p(I,J)/\sum_K p(I,K)$.

I,J	G	A	T	C	$\sum_j P(I,J)$
G	0.1042	0.0644	0.0511	0.0664	0.2860
A	0.09193	0.10010	0.04902	0.04494	0.2860
T	0.07660	0.03166	0.05515	0.04392	0.2073
C	0.01327	0.08988	0.05311	0.06435	0.2206
$\sum_{ip} P(I,J)$	0.2860	0.2860	0.2073	0.2206	

II. THEORETICAL MODEL

Our Hamiltonian is an effective tight-binding model describing one electron moving in a chain with a single orbital per site and nearest-neighbor interactions, i.e. [17],

$$t(\psi_{j+1} + \psi_{j-1}) = (E - \epsilon_j)\psi_j, \quad (1)$$

where ϵ_j is the single energy at the orbital ψ_j , whereas t is the common first-neighbor electronic overlap (hopping amplitude).

Within this framework, the (discrete) Schrödinger equation can be written as

$$\begin{pmatrix} \psi_{j+1} \\ \psi_j \end{pmatrix} = M(j) \begin{pmatrix} \psi_j \\ \psi_{j-1} \end{pmatrix}, \quad (2)$$

where $M(j)$ is the transfer matrix

$$M(j) = \begin{pmatrix} (E - \epsilon_j)/t & -1 \\ 1 & 0 \end{pmatrix}. \quad (3)$$

After successive applications of the transfer matrices we have

$$\begin{pmatrix} \psi_{j+1} \\ \psi_j \end{pmatrix} = M(N)M(N-1)\cdots M(2)M(1) \begin{pmatrix} \psi_1 \\ \psi_0 \end{pmatrix}. \quad (4)$$

In this way we have the wave function at an arbitrary site. Calculating the product of transfer matrices is completely equivalent to solving the Schrödinger equation for the system. The criterion for allowed energy is when $(1/2)\text{Tr}[\mathcal{P}] < 1$, with $\text{Tr}[\mathcal{P}]$ meaning the trace of the matrix \mathcal{P} , and $\mathcal{P} = M(N)M(N-1)\cdots M(2)M(1)$ [18].

For the DNA sequence of the first sequenced human chromosome 22 (Ch22), entitled NT_{011520} , the number of letters of this sequence is about 3.4×10^6 nucleotides. This sequence was retrieved from the internet page of the National Center of Biotechnology Information. The energies ϵ_j are chosen from the ionization potential of the respective nucleotides [19], i.e., $\epsilon_A = 8.24$, $\epsilon_T = 9.14$, $\epsilon_C = 8.87$, and $\epsilon_G = 7.75$, all in eV, representing the adenine, guanine, thymine, and cytosine molecules. We will consider finite segments of the Ch22 chromosome starting at the 1500th nucleotide.

In what follows we will focus on the electronic transport considering the above tight-binding Hamiltonian model [Eq. (1)] for a single-strand DNA sequence. We are aware that in order to model specific transport properties of DNA molecules, it would be important to consider not only their

double-strand character, whose electronic localization has been recently investigated [20,21], but also the different values assumed by the coupling constant between distinct pairs of nucleotides [22–24], which in turn has important consequences in the on-site (ionization) energies ϵ_j [25]. However, we believe that the relative role played by long- and short-range correlations in the nucleotide sequence can be analyzed in great detail using the proposed single-strand model used here, with correlated diagonal disorder.

To set up a quasiperiodic chain of Rudin-Shapiro type, we consider that the energies ϵ_j take four different values ϵ_G , ϵ_A , ϵ_C , and ϵ_T as in the DNA genomic sequence. With the intention of comparing this sequence with the genomic one, we assume that their numerical values are the same. Starting from a G (guanine) nucleotide as seed, the quasiperiodic RS sequence can be built through the inflation rules $G \rightarrow GC$, $C \rightarrow GA$, $A \rightarrow TC$, and $T \rightarrow TA$. The RS sequence belongs to the family of so-called substitutional sequences, which are characterized by the nature of their Fourier spectrum. It exhibits an absolutely continuous Fourier measure, a property that it shares with random sequences [26]. It should be contrasted with the Fibonacci sequence (another substitutional sequence) which displays a dense pure point Fourier measure, characteristic of a true quasicrystal-like structure (for a review of the physical properties of these and others quasiperiodic structures, see Ref. [27]). This important difference has been discussed in the literature in connection with the localization properties of both elementary excitations [28] and classical waves [29] in the RS sequence, as compared to other substitutional sequences.

We also constructed a random sequence containing the same pair correlation of the Ch22 chromosome sequence. To this end we first measured the fraction of pairs $p(I,J)$ ($I, J = G, A, C$, and T) in the Ch22 sequences considered. The results for these conditional probabilities are summarized in Table I for a representative sequence. After that, we generate an artificial sequence starting with a cytosine (C) site. During the sequence construction, the nucleotide following a type I nucleotide is chosen to be of type J with probability $P(J,I) = p(I,J)/\sum_K p(I,K)$. The resulting pair-correlated sequence (we call it the PC sequence) has only short-range correlations which, by construction, are the same as the original Ch22 sequence.

To compare some statistical properties of the above sequences, we compute the autocorrelation function of the potential landscape of segments of Ch22 and RS and PC sequences as a function of the number of nucleotides (see Fig.

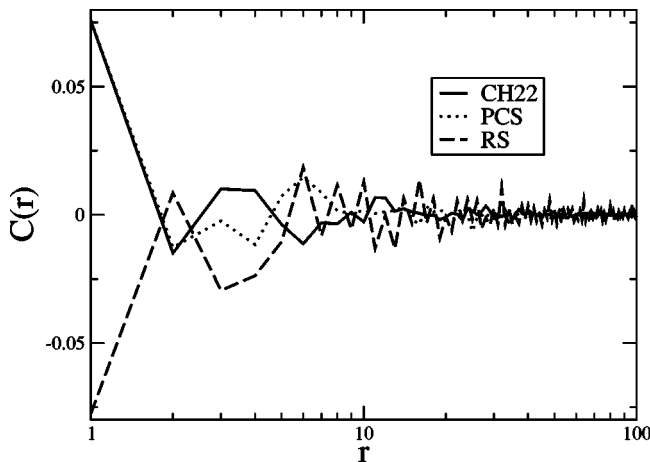


FIG. 1. Autocorrelation of segments of Ch22, RS, and PC sequences. The oscillations observed for the RS sequence reflect its antipersistent character. Notice that it is longer-ranged correlations as compared to the Ch22 sequence. The PC sequence has the same first-neighbor correlations as the Ch22 sequence but is shorter-range correlated.

1). Note that by construction the PC sequence has the same first-neighbor correlation as the Ch22 sequence. The RS sequence has a clear signature of antipersistent correlations reflected in the oscillatory behavior of its autocorrelation. Besides that, the amplitudes of the RS correlations are consistently larger than those in the Ch22 and PC sequences. On the other hand, the PC sequence is shorter ranged than the actual Ch22 sequence.

Another important statistical characterization of random sequences is the rescaled range statistical analysis, introduced by Hurst *et al.* [30]. It provides a sensitive method for revealing long-run correlations in random processes. Given a nucleotide sequence of size L , the rescaled range statistics for a discrete random walk, whose steps are ξ_i is defined as follows. First, one defines rescaled variables

$$X(k,n) = \sum_{u=1}^k (\xi_u - \langle \xi \rangle_n), \quad (5)$$

where $\langle \xi \rangle_n$ is the mean value after n steps ($1 \leq n \leq L$), i.e.,

$$\langle \xi \rangle_n = \frac{1}{n} \sum_{i=1}^n \xi_i. \quad (6)$$

The range $S(n)$ for a random walk of lengths n is then given by

$$S(n) = \max[X(k,n)] - \min[X(k,n)], \quad (7)$$

for $1 \leq k \leq n$. The scaled range function $R(n)$ is therefore

$$R(n) = S(n)/\sigma(n), \quad (8)$$

where $\sigma^2(n)$ is the standard deviation of ξ_i over walks of lengths n , and averaged over the entire sequence, i.e.,

$$\sigma^2(n) = \frac{1}{n} \sum_{i=1}^n (\xi_i - \langle \xi \rangle_n)^2. \quad (9)$$

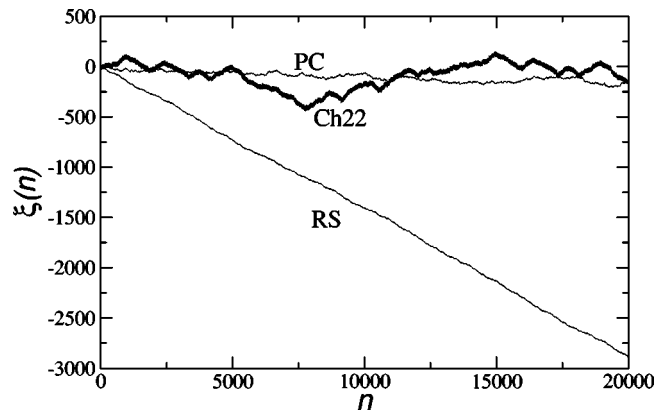


FIG. 2. Random walks generated from segments of Ch22, RS, and PC sequences. The larger variance of the Ch22 sequence is related to its long-range persistent behavior.

To perform the rescaled range analysis of the Ch22, RS, and PC sequences, we constructed auxiliary random walks initiated from the first to the last nucleotide of the sequences with the following rule: for a purine (A, G) the walker steps down and $\xi_i = -1$; for a pyrimidine (T, C) the walker steps up and $\xi_i = +1$. After n steps, the displacement is $\xi(n) = \sum_{i=1}^n \xi_i$. The resulting random walks for Ch22, RS, and PC sequences are shown in Fig. 2, where we have plotted $\xi(n)$ as a function of the number of steps n . Note that for the RS sequence the drift to negative values is stronger than in both Ch22 and PC sequences, since it contains a larger fraction of purines.

Many processes in nature are not independent, but show significant long-term correlations. In this case the asymptotic scaling law is modified and $R(n)$ is asymptotically given by a power law n^H , where H is the so-called Hurst exponent. Feller [31] has proved that the asymptotic behavior for any independent random process with finite variance is given by $R(n) = (n\pi/2)^{1/2} - 1$, which yields a Hurst exponent $H = 0.5$

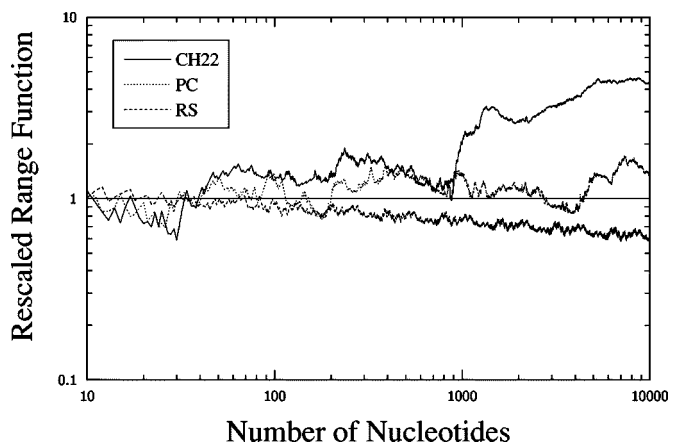


FIG. 3. Log-log plot of the rescaled range function $R(n)$, normalized to the one associated with a noncorrelated sequence, versus n for the Ch22, Rudin-Shapiro, and PC sequence random walks. RS and PC sequences have rescaled range functions relatively close to that expected for an uncorrelated random walk. However, the RS walk depicts a small antipersistence while the PC exhibits some persistence as in the Ch22 walk.

(the ordinary Brownian motion). A *persistent* behavior is characterized by a Hurst exponent $0.5 < H < 1$, while an *antipersistent* one is characterized by $0 < H < 0.5$. Many examples of natural phenomena that show persistent behavior can be found in [32].

In Fig. 3 we plot on a log-log scale the rescaled range function $R(n)$, normalized to the one associated with a non-correlated sequence given by $R(n) = (n\pi/2)^{1/2} - 1$, as a function of the number of nucleotides n for the genomic DNA, Rudin-Shapiro, and PC sequences. The straight line corresponds to the case of a completely uncorrelated random walk ($H=0.5$). From there, we can see clearly that in the genomic DNA random walk the asymptotic behavior is persistent, while for the Rudin-Shapiro sequence the random walks are antipersistent. On the other hand, the rescaled range function for the PC sequence oscillates around an exact power law for

a small number of nucleotides, becoming persistent with a minor deviation from the Ch22 behavior as the number of nucleotides increases.

III. CONDUCTIVITY AND WAVE-PACKET DYNAMICS

Consider now that the above sequences are further assumed to be connected to two semi-infinite electrodes whose energies ϵ_m are adjusted to simulate a resonance with the guanine highest occupied molecular orbital energy level, i.e., $\epsilon_m = \epsilon_G$. The hopping integrals are chosen such that $t_m = t = 1$ eV, although *ab initio* calculations suggest that $t_m \approx 0.1-0.4$ eV. For this system, the transmission coefficient $T_N(E)$, which gives the transmission rate through the chain and is related to the Landauer resistance, is defined by [33]

$$T_N(E) = \frac{4 - X^2(E)}{\left[-X^2(E)(\mathcal{P}_{12}\mathcal{P}_{21} + 1) + X(E)(\mathcal{P}_{11} - \mathcal{P}_{22})(\mathcal{P}_{12} - \mathcal{P}_{21}) + \sum_{i,j=1,2} \mathcal{P}_{ij}^2 + 2 \right]}, \quad (10)$$

where $X(E) = (E - \epsilon_m)/t_m$, and \mathcal{P}_{ij} are elements of the transfer matrix \mathcal{P} . For a given energy E , $T_N(E)$ measures the level of backscattering events in the electron (or hole) transport through the chain.

In Fig. 4 we plot the transmission coefficient $T_N(E)$, as given by Eq. (10), as a function of the energy, in units of eV, for the DNA Ch22 sequence with the number of nucleotides

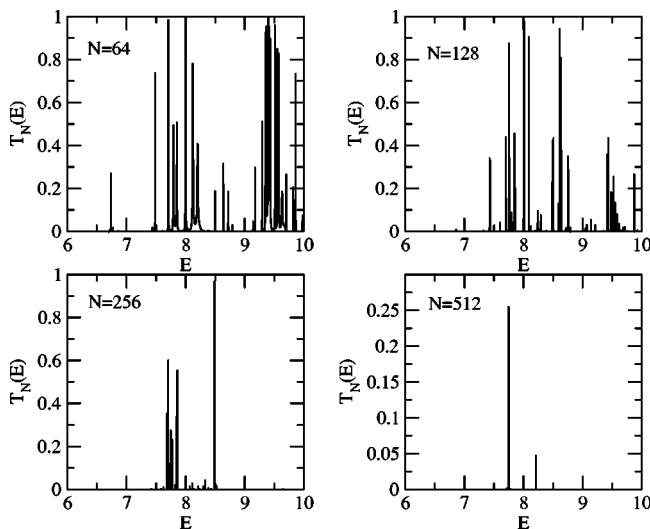


FIG. 4. Transmittance coefficient $T_N(E)$ as a function of the energy E , in units of eV, for Ch22-based sequence near the band center, for the number of nucleotides N equal to 64, 128, 256, and 512. Notice that the transmission bands shrink as the segment size increases. However, the presence of correlations contributes to the survival of resonant transmission peaks for sequences up to hundreds of nucleotides.

(N) equal to 64, 128, 256, and 512, respectively. Observe that the transmission bands in the spectra becomes more and more fragmented as the segment size increases. This feature is related to the localized nature of the one-electron eigenstates in disordered chains. It is relevant to stress that the presence of long-range correlations in the disorder distribution was recently shown to be a possible mechanism to induce delocalization in low-dimensional systems. However, the actual correlations in DNA sequences are not strong enough to produce this correlation-induced transition and the stationary states remain all localized. However, the presence of long-range correlations enhances the localization length and, therefore, transmission resonances survive in larger segments as compared with a noncorrelated random sequence. To illustrate this correlation effect we plot in Fig. 5 the transmission coefficient for long-range correlated Rudin-Shapiro sequences, for the same number of nucleotides N as in Fig. 4. The transmission spectra depict a trend similar to the one produced by the genomic sequence. The transmission spectra derived from the PC sequence (not shown) also exhibit the same pattern, with the transmission resonances being more sensitive to increases of the segment size due to the short-range character of its correlations.

To compare the transmittance properties of different chains, the behavior of the Lyapunov coefficient

$$\gamma_N(E) = (1/2N) \ln[|T_N(E)|] \quad (11)$$

is plotted in Figs. 6 and 7, as a function of the energy E , in units of eV, for Ch22-based and Rudin-Shapiro sequences with $N=64, 128, 256,$ and 512 , respectively. This exponent, for a system with uncorrelated disorder, is related to the localization length $\lambda(E)$ by [33]

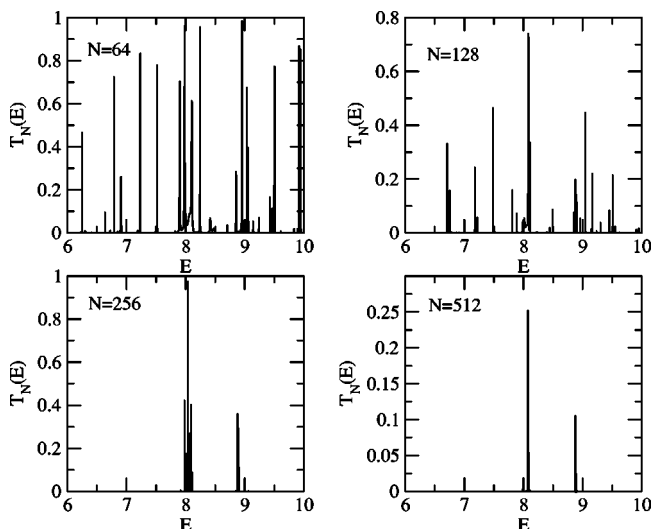


FIG. 5. As in Fig. 4 but for Rudin-Shapiro sequence. Observe a similar trend to the one depicted in Fig. 4. This feature supports the relevance of correlations in the nucleotide distribution to the survival of transmission resonances on finite segments irrespective of its persistent or antipersistent nature.

$$\lambda(E) = \left[\lim_{N \rightarrow \infty} \gamma_N(E) \right]^{-1}. \quad (12)$$

In addition, in the presence of scale invariance properties, the underlying structure of $\gamma_N(E)$ reflects the self-similarity of the spectrum.

Focusing now on the wave-packet dynamics in the above finite segments, we solved numerically the time-dependent Schrödinger equation and computed the time dependence of the *spread* of the wave function (square root of the mean squared displacement), as a function of time, by using

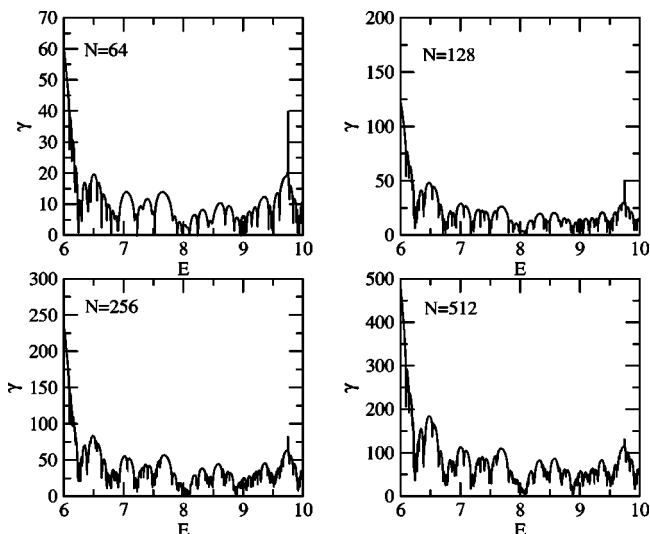


FIG. 7. As in Fig. 6 but for Rudin-Shapiro sequence. The underlying structure is similar to the one presented for the actual Ch22 sequence.

$$\sigma(t) = \sqrt{\sum_{n=1}^N [n - \langle n(t) \rangle]^2 |\psi_n(t)|^2}. \quad (13)$$

Starting from a wave packet localized at the guanine (G) site closest to the center of segments with 10^4 nucleotides, the spread of the wave function is depicted in Fig. 8 for the Ch22, RS, PC, and uncorrelated sequences. For the uncorrelated random sequence we considered the same fraction of each nucleotide composing the Ch22 sequence under consideration. The root mean square displacement $\sigma(t)$ on Ch22

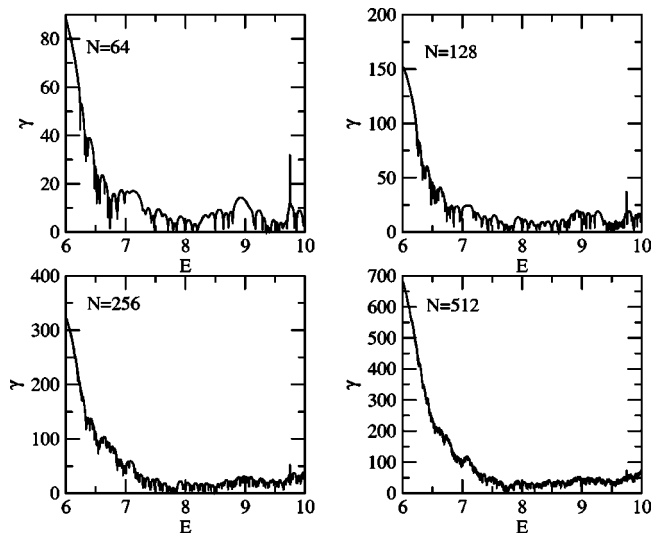


FIG. 6. Lyapunov coefficient $\gamma_N(E)$ as a function of the energy E , in units of eV, for Ch22-based sequence. We have also considered the number of nucleotides N equal to 64, 128, 256, and 512. The underlying structure emerging at large sequences reflects some degree of self-similarity of the transmission spectra.

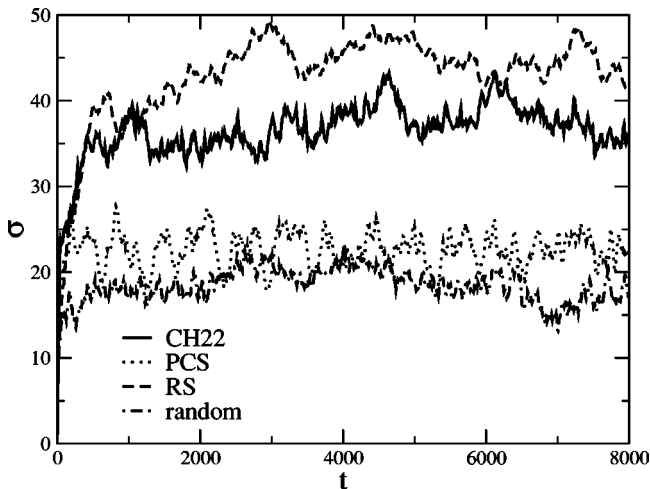


FIG. 8. Spread of the wave function (square root of the mean squared displacement) σ given by Eq. (13) as a function of time. The wave-packet dynamics on Ch22, PC, fully uncorrelated random (averaged over ten distinct segments of 10^4 nucleotides), and RS sequences were considered. The anomalous spread on Ch22 is twice as large as that in the uncorrelated sequence. However, the long-range correlations in the RS sequence overestimate the wave function spread. The pair correlations account for $\sim 50\%$ of the anomalous spread in the Ch22 sequences.

segments displays an initial ballistic spread but saturates at a finite value due to the localized nature of the one-electron eigenstates. The saturation value is of the order of $\sigma=30$ for the Ch22 segments. This value is twice the one reached for the fully uncorrelated random sequence, thus indicating that correlations in the nucleotide distribution play a significant role in the wave-packet dynamics. On the other hand, the spread on the RS sequence overpasses that for the actual Ch22 by $\sim 50\%$. This fact is related to the longer-range character of its correlations as already discussed (see Fig. 1). Notice, however, that the spread in the PC sequence is only $\sim 25\%$ below that of Ch22 segments, which seems to indicate that a well controlled approach to the actual wave-packet dynamics on DNA segments can be obtained by including further short-range correlations.

IV. CONCLUSIONS

Over the past few years, bionanomaterial science has emerged as an exciting field in which theoretical and experimental studies of nanobiostructures have stimulated a broader interest in developing the field of nanometer-scale electronic devices. In particular, intelligent composite biological materials have become an interdisciplinary frontier in life science and material science. Nevertheless, the construction of nanometer-scale circuits remains problematic, and the use of molecular recognition processes and the self-assembly of molecules into supramolecular structures might help overcome these difficulties. In this context, the ability to choose the sequence of nucleotides, and hence provide addressability during the self-assembly processes, besides its inherent

molecular recognition, makes DNA an ideal molecule for these applications.

Aiming to further contribute to the present understanding of the role played by correlations on the electronic properties of DNA segments, we have studied here the electronic transport properties of finite sequences of nucleotides within a tight-binding approach of single-strand DNA sequences with pure diagonal correlated disorder. In order to reveal the actual relevance of short- and long-range correlations, we compared the transmission spectra and the wave-packet spread on segments of the Ch22 human chromosome with those resulting from the quasiperiodic Rudin-Shapiro sequence as well as from a pair-correlated sequence. We obtained that the long-range correlations present in Ch22 and RS sequences are responsible for the slow vanishing of some transmission peaks as the segment size is increased, which may promote an effective electronic transport at specific resonant energies of finite DNA segments. On the other hand, much of the anomalous spread of an initially localized electron wave packet can be accounted for by short-range pair correlations on DNA. This finding suggests that a systematic approach based on the inclusion of further short-range correlations on the nucleotide distribution can provide an adequate description of the electronic properties of DNA segments.

ACKNOWLEDGMENTS

We would like to acknowledge partial financial support from CNPq, MCT-NanoSemiMat, and FINEP-CTInfra (Brazilian Research Agencies) as well as from FAPEAL (Alagoas State Research Agency).

-
- [1] *Future Trends in Microelectronics: The Road Ahead*, edited by S. Luryi, J. M. Xu, and A. Zaslavsky (Wiley, New York, 1999).
- [2] R. G. Endres, D. L. Cox, and R. R. P. Singh, *Rev. Mod. Phys.* **76**, 195 (2004).
- [3] Y. Asai, *J. Phys. Chem. B* **107**, 4647 (2003).
- [4] S. V. Rakhmanova and E. M. Conwell, *J. Phys. Chem. B* **105**, 2056 (2001).
- [5] H. W. Fink and C. Schönberg, *Nature (London)* **398**, 407 (1999).
- [6] Y. Okahata, T. Kobayashi, K. Tanaka, and M. Shimomura, *J. Am. Chem. Soc.* **120**, 6165 (1998).
- [7] F. D. Lewis, T. F. Wu, Y. F. Zhang, R. L. Letsinger, S. R. Greenfield, and M. R. Wasielewski, *Science* **277**, 673 (1997).
- [8] G. Taubes, *Science* **275**, 1420 (1997).
- [9] A. J. Storm, J. van Noort, S. deVries, and C. Dekker, *Appl. Phys. Lett.* **79**, 3881 (2001).
- [10] D. Porath, A. Bezryadin, S. deVries, and C. Dekker, *Nature (London)* **403**, 635 (2000).
- [11] A. Yu. Kasumov, D. V. Klinov, P.-E. Roche, S. Guéron, and H. Bouchiat, *Appl. Phys. Lett.* **84**, 1007 (2004).
- [12] E. Braun, Y. Eichen, U. Sivan, and G. Ben-Yoseph, *Nature (London)* **391**, 775 (1999).
- [13] C. Treadway, M. G. Hill, and J. K. Barton, *Chem. Phys.* **281**, 409 (2002).
- [14] F. A. B. F. de Moura and M. L. Lyra, *Phys. Rev. Lett.* **81**, 3735 (1998).
- [15] P. Carpena, P. B-Galván, P. Ch. Ivanov, and H. E. Stanley Nature (London) **418**, 955 (2002); **421**, 764 (2003).
- [16] S. Roche, *Phys. Rev. Lett.* **91**, 108101 (2003).
- [17] M. Kohmoto, L. P. Kadanoff, and C. Tang, *Phys. Rev. Lett.* **50**, 1870 (1983).
- [18] P. W. Mauriz, E. L. Albuquerque, and M. S. Vasconcelos, *Physica A* **294**, 403 (2001).
- [19] H. Sugiyama and I. Saito, *J. Am. Chem. Soc.* **118**, 7063 (1996).
- [20] H. Yamada, *Int. J. Mod. Phys. B* **18**, 1697 (2004).
- [21] K. Iguchi, *J. Phys. Soc. Jpn.* **70**, 593, (2001); *Int. J. Mod. Phys. B* **11**, 2405 (1997).
- [22] H. Sugiyama and I. Saito, *J. Am. Chem. Soc.* **118**, 7063 (1996).
- [23] A. A. Voityuk, J. Jortner, M. Bixon, and N. Rosch, *J. Chem. Phys.* **114**, 5614 (2001).
- [24] Y. J. Yan and H. Zhang, *J. Theor. Comput. Chem.* **1**, 225, (2002).
- [25] Y. A. Berlin, A. L. Burin, and M. A. Ratner, *Superlattices Microstruct.* **28**, 241 (2000).

- [26] F. Axel, J. P. Allouche, and Z. Y. Wen. *J. Phys.: Condens. Matter* **4**, 8713 (1992).
- [27] E. L. Albuquerque and M. G. Cottam, *Phys. Rep.* **376**, 225 (2003).
- [28] M. Dulea, M. Johansson, and R. Riklund, *Phys. Rev. B* **45**, 105 (1992); **46**, 3296 (1992); **47**, 8547 (1993).
- [29] H. Aynaou, V. R. Velasco, A. Nougouai, E. H. El Boudouti, B. Djafari-Rouhani, and D. Bria, *Surf. Sci.* **538**, 101 (2003).
- [30] H. E. Hurst, R. Black, and Y. M. Sinaika, *Long-Term Storage in Reservoir: An Experimental Study* (Constable, London, 1965).
- [31] W. Feller, *Am. Math. Stat.* **22**, 427 (1951).
- [32] J. Feder, *Fractals* (Plenum Press, New York, 1988).
- [33] S. Roche, D. Bicout, E. Maciá, and E. Kats, *Phys. Rev. Lett.* **91**, 228101 (2003); **92**, 109901 (2004).